Colloid & Polymer Science Colloid Polym Sci 272:1252–1258 (1994)

Adsorption behavior of bis (2-ethylhexyl) sodium sulfosuccinate (AOT) at the mercury-electrolyte solution interface as a function of electrode potential and time

A. Avranas, N. Papadopoulos, and S. Sotiropoulos

Laboratory of Physical Chemistry Department of Chemistry, Aristotle University, Thessaloniki, Greece

Abstract: The dependence of the differential capacitance (C) of the electrode double layer of a hanging mercury drop electrode in bis (2-ethylhexyl) sodium sulfosuccinate (AOT) solutions on electrode potential (E) and time is measured using three-dimensional phase sensitive ac voltammetry. This methodology, possessing a very wide time window that permits a detailed study of the adsorption phenomena, is based on the reconstruction of C vs E curves, sampled after many phase-sensitive ac chronoamperometric experiments. The shape of these curves allows an estimation of the structure of the layer of AOT molecules adsorbed at the electrode surface. AOT molecules form micelles in bulk solutions and they also associate in the charged interface under the strong influence of the electric field into surface aggregates which depend on their concentration and applied potential. The presence of AOT micelles in the bulk solution can be linked with the appearance of a surface film at potentials more negative than those corresponding to a condensed film linked with a capacitance value slightly higher than that normally attributed to a compact layer. The whole phenomenon is proved to be very dependant upon time.

Key words: Adsorption – AOT – differential capacitance – three-dimensional voltammetry

Introduction

Sulfosuccinates, mainly in the form of bis (2-ethylhexyl) sodium sulfosuccinate (Aerosol OT hereafter referred to as AOT) are used extensively as wetting and emulsifying agents and in the process of enhanced oil recovery [1]. Two-tailed surfactants, especially if the carbon chains are quite long, are generally thought to form bilayer vesicles in water while single-tailed surfactants form spherical micelles [2–4].

Although AOT is well characterized in non-aqueous solvents as a bilayer vesicle [5–6], conductance and fluorescence quenching methods argue for the formation of near spherical micelles beyond the CMC in aqueous solutions of sulfosuccinates [7]. Surface tension data [8, 9], conductance data [10], and NMR studies [11] all suggest the formation of micelles of small aggregation numbers.

Another interesting feature of the interfacial behavior of sulfosuccinates in the water-aqueous solution interface is the slow attainment of the adsorption equilibrium [12] and the corresponding slow surface tension changes could be ascribed to changes in tilt angle for raw of molecules [13].

The interfacial behavior of AOT at the ideally polarized-charged interface between a mercury electrolytic solution has not been studied yet. Such a study would be of interest in order to investigate whether a micelle-forming surfactant (which at even higher concentrations exists in different phases [10,13,14]) retains its associative character under the strong influence of the electric field. One could also test whether slow changes in the adsorption state still occur under the strong orientation forces that prevail at a charged interface. The adsorption of AOT on mercury should cause a change in the electrode's double-layer differential capacitance, as a result of the replacement of counter-ions and water molecules from the electrode surface by surfactant molecules from the solution. Many works have been published on the adsorption of bulk micelle forming surfactants on mercury by means of differential capacitance measurements which try to find a correlation between the properties of the differential capacitance (C) vs applied potential (E) curves and the bulk CMC value [15–19].

Phase changes, such as those expected for AOT on the mercury surface, are often kinetically hindered processes [20, 21]. Furthermore, the need to study the influence of time on the adsorption of AOT on mercury is obvious since the surface tension of aqueous solutions of AOT shows a slow equilibration. Therefore, the use of a dropping mercury electrode, DME, which has a limited drop lifetime, or of a hanging mercury drop electrode, HMDE, using semistatic ac voltammetry would not be adequate in studying the equilibrium properties of the system. A fully automated methodology, whose principle lies in current sampled voltammetry, has been developed in our laboratory [22–26] and allows the study of slowly proceeding phase changes almost continuously up to the point of equilibrium. This method, named three-dimensional phase-sensitive ac voltammetry (3D/ac/V), is based on the reconstruction of the differential capacitance C vs. applied potential E curves for selected time values t. The C vs E curves constructed for relatively long periods provide the equilibrium situation, whereas those at intermediate times provide information about the time evolution of the phenomenon.

The aim of the present work is to study the association of AOT on the Hg/electrolytic solution interface and how this changes in time. A correlation (if any) between the CMC value of the aqueous AOT solutions and the picture of the C vs E curves will also be sought.

Experimental

The AOT with a purity greater than 98% was obtained from Fluka and did not show a minimum in the surface tension near the critical micellar concentration, indicating the absence of surface active impurities. The surface tension measurements were obtained following the Wilhelmy plate method using Kruess K10 digital tensiometer and the solutions were allowed to stand until equilibrium was reached. Na_2SO_4 was obtained from Fluka (puriss p.a. 99.5%) and served as supporting electrolyte (0.1 M). All experiments were performed at 25 °C using AOT concentrations ranging from 10^{-5} to 10^{-2} M, i.e., above and below its CMC.

The capacitive current I_c was recorded by means of phase-sensitive ac chronoamperometry using a PAR Model 170 electrochemistry system interfaced to an AT compatible (VIP 200 12 MHz) via a 14-bit AD/DA card using a standard three-electrode cell arrangement. Each mercury drop was formed on a HMDE, the working electrode, within a period of 3 s at -1.75V vs SCE (to which all potentials in this paper are referred), where preliminary experiments for short drop times showed a limited adsorption. Experimental details are given in Ref. [25].

Results

The C-E-t surface for 5×10^{-5} M AOT in 0.1 M Na_2SO_4 is given in Fig. 1, and it can be seen that it provides an overall picture of the whole adsorption process.

The differential capacitance vs. applied potential curves of the double layer formed between the polarized hanging mercury electrode and aqueous solutions of four different AOT concentrations are shown in Fig. 2 for selected time values in the 0.5–30 s range. They are constructed from isochronous capacitance data sampled after a potential step has been applied to the electrode from -1.75 V (no adsorption occurring) to the value of interest, during many ac phase-sensitive chronoamperometric experiments. These curves resemble typical ac voltammograms. Figure 3a shows a classic C vs E curve recorded on a single mercury drop during a potential sweep experiment, and Fig. 3b gives the C vs E curve obtained by 3D/ac/V at intermediate times (5 s).

The general feature of the equilibrium curves ($t \geq 15$ s for concentrations $\geq 5 \times 10^{-5}$ M, Figs. 2b–d) is the appearance of a wide capacitance pit

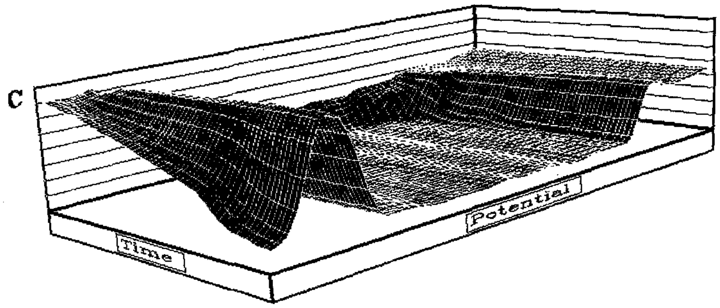

Fig. 1. C-E-t surface for 5×10^{-5} M AOT aqueous solution in 0.1 M Na_2SO_4

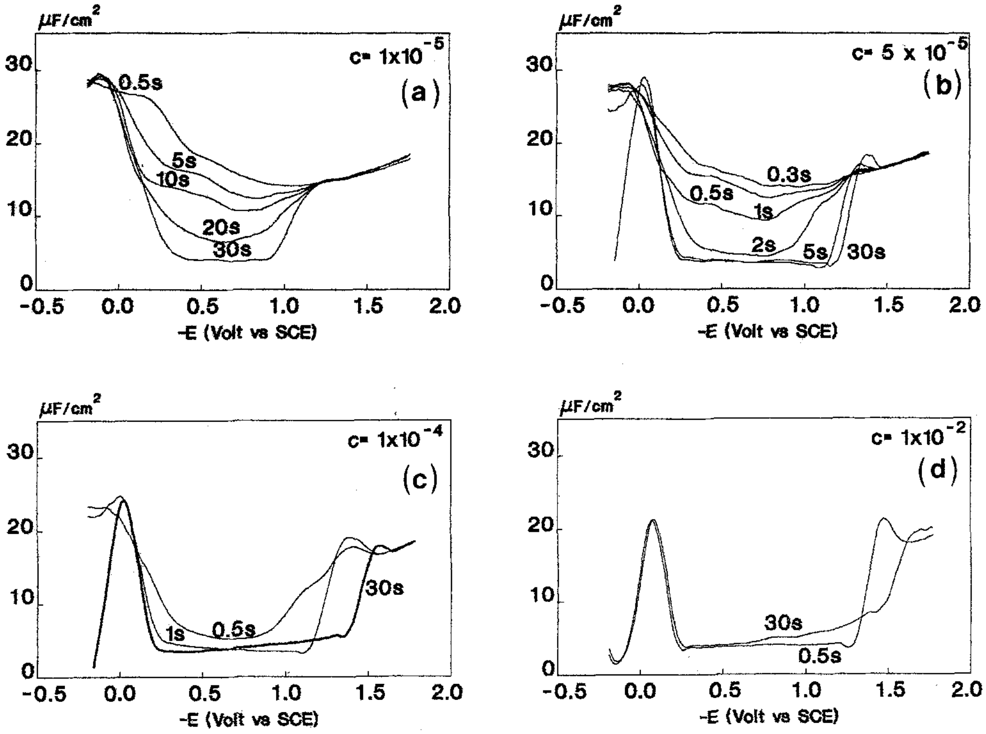

Fig. 2. Differential capacitance vs. applied potential curves, for selected time periods, of the interface formed between a HMDE and 0.1 M Na_2SO_4 aqueous solutions of AOT

(~ $4 \mu F/cm^2$) surrounded by a rather steep peak at far negative polarizations (c.a. − 1.5 V) and a wide peak at positive polarizations (c.a. 0 V). For the two higher concentrations (Figs. 2c, d) the central pit is transformed at c.a. − 1.0 V into a slightly higher plateau before the cathodic peak is observed.

Although in the far cathodic region, at polarizations more negative than − 1.6 V, AOT is desorbed (as indicated by the coincidence of all the curves with that of the supporting electrolyte), this is not the case at very positive polarizations. That is, at potentials higher than 0 V there is a large decrease of the differential capacitance.

Figure 4 shows surface tension data of aqueous AOT solutions containing 0.1 M Na_2SO_4 determined by the plate method, using Kruess K10 digital tensiometer. These data show a CMC value of 3×10^{-4} M, while CMC values from 2.5 to 6×10^{-3} are reported in the literature for the AOT aqueous solutions [8,10].

Figures 5–8 show C vs t curves recorded when the potential of the HMDE in contact with a 5×10^{-5} M solution of AOT was stepped

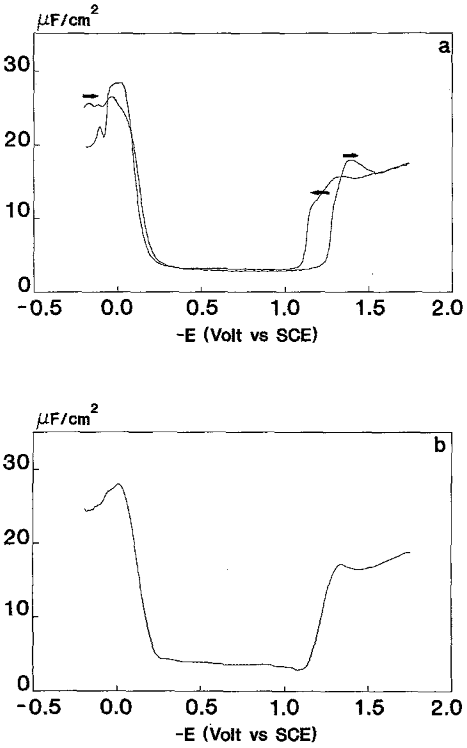

Fig. 3. Differential capacitance vs. Applied potential curves recorded on an HDME in contact with a 5×10^{-5} M AOT and 0.1 M Na_2SO_4 aqueous solution by means of a) a potential sweep experiment at 50 mV/s and b) capacitance data sampled at 5 s after the application of a pulse to a given potential

from -1.75 V vs SCE to the potential value of interest.

Discussion

An alternative approach to micellization at charged interfaces based on statistical and classical thermodynamics has recently been introduced in our laboratory [27, 28]. An interpretation of the behavior of a few systems according to that approach has also been attempted [29, 30]. The basic idea of this treatment is that micelle formation at a charged interface is a phase transition between a condensed or a non-saturated state of the interface and the micellar phase. The position and shape of the capacitance peaks that correspond to these transitions strongly depend on the size of micelles and the existence of metastable states, whereas the presence of deformed peaks is

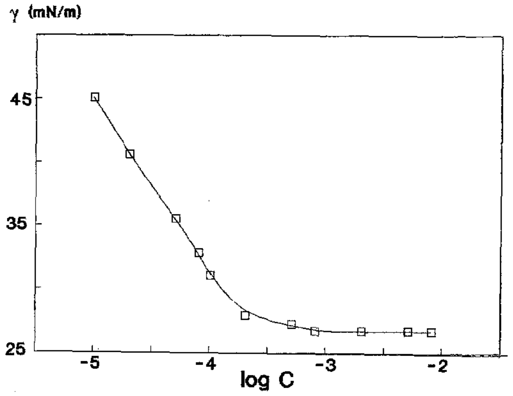

Fig. 4. Surface tension vs. the logarithm of molar concentration of AOT aqueous solutions in the presence of 0.1 M Na_2SO_4

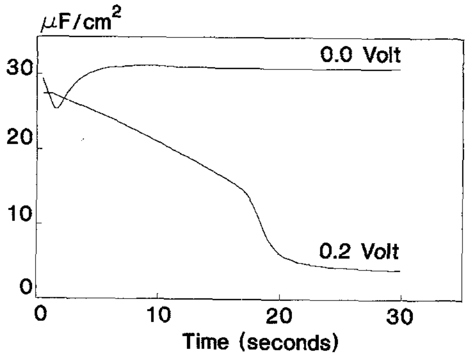

Fig. 5. Capacitance transients recorded after the potential of the HMDE in contact with a 5×10^{-5} M AOT and 0.1 M Na_2SO_4 aqueous solution was stepped to $+0.2$ and 0 V vs. SCE

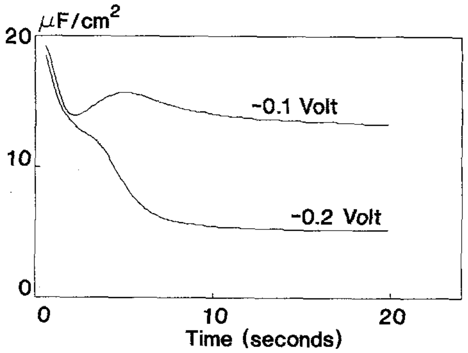

Fig. 6. Capacitance transients recorded after the potential of the HMDE in contact with a 5×10^{-5} M AOT and 0.1 M Na_2SO_4 aqueous solution was stepped to -0.1 and -0.2 V vs. SCE

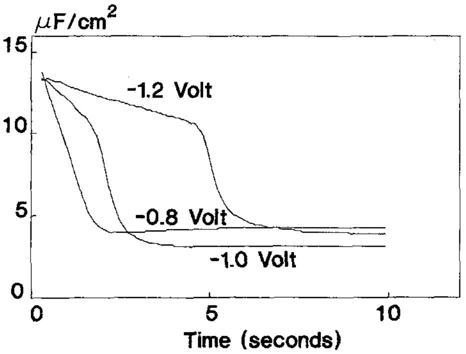

Fig. 7. Capacitance transients recorded after the potential of the HMDE in contact with a 5×10^{-5} M AOT and 0.1 M Na_2SO_4 aqueous solution was stepped to -0.8, -1.0 and -1.2 V vs. SCE

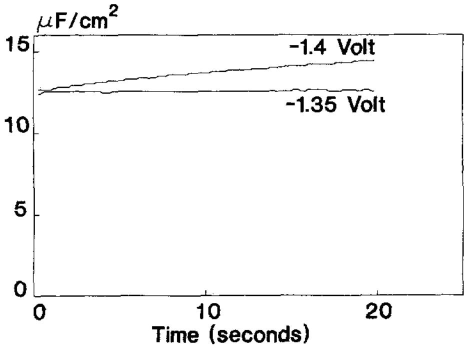

Fig. 8. Capacitance transients recorded after the potential of the HMDE in contact with a 5×10^{-5} M AOT and 0.1 M Na_2SO_4 aqueous solution was stepped to -1.350 and -1.40 V vs. SCE

a sufficient but not necessary criterion for phase transformations within successive layers of the interface [27–30]. We believe that this extremely deep capacitance "well" at c.a. $+0.2$ V corresponds to the formation of a polylayer (or at least) a bilayer of AOT anions. Polylayer formation has also been observed for other anionic micelle forming surfactants at positive potentials [24, 29] and cationic ones at negative potentials [23]. Polylayer formation by AOT at these potentials ($+0.2$ V) is strongly supported by the fact that the capacitance of the corresponding state keeps on falling with increasing surfactant bulk concentration (from 4 to 2 $\mu F/cm^2$ when one passes from 5×10^{-5} to 10^{-2} M AOT, Fig. 2). At a molecular level, we believe that at those extremely positive polarizations, AOT monomers are adsorbed with their negatively charged sulfonic groups adjacent to the electrode surface and a monolayer of closely packed monomers with their hydrophobic tails towards the solution side of the interface is formed first. Then, more AOT molecules arrive at the interface and a second layer is gradually being built up on top of the first layer. The orientation of the molecules of the second layer is more likely to be opposite of that of the first one. That is, they probably have their charged $-SO_3^-$ groups towards the solution and their hydrophobic parts interacting with those of the molecules of the first monolayer.

The interactions can be both hydrophobic ones and hydrogen bonding through the carbonyl groups of AOT. Such interactions are wellknown to form bilayer AOT vesicles in both solutions [7].

The central capacitance pit most probably corresponds to a condensed state of the interface since it shows many of the general characteristics of C vs E curves attributed to compact layers [31,32] (Fig. 2). That is, it has a very low capacitance value (c.a. $4 \mu F/cm^2$) extended over a wide potential range; its limits show hysterisis loops in classic voltammetric experiments (Fig. 3a), and it is surrounded by steep (at least at negative potentials) and concentration independent peaks. The AOT molecules are most probably with their charged groups towards the solution and their hydrocarbon groups interacting with the hydrophobic Hg surface [24,29], i.e., with an opposite orientation from that in the first layer of the polylayer present at $+0.2$ V.

The reason why the compact layer is apparently destroyed at positive polarizations through a "bell-shaped" peak instead of a sharp "needle-like" peak as expected for a phase transition occurring in a single layer [28], is that the abovementioned peak is the result of two different phase transitions at neighboring potentials. The first one (at the cathodic part of the anodic peak) corresponds to a phase transition between a condensed AOT monolayer and a non-saturated surface solution of AOT monomers. However, as the potential becomes more positive the AOT molecules are not desorbed, but there occurs phase transition of the non-saturated surface solution into a polylayer (anodic branch of the anodic peak) as described above. The fact that the decomposition of the compact layer may be realized through a series of transformations into aggregates ("surface micelles") is also expected to "smooth" the anodic branch of the peak. It is interesting that two overlapping peaks at negative polarizations (one corresponding to the dissolution of the compact film and the other to the subsequent polylayer formation) can be seen for intermediate times or during relatively fast potential sweep experiments (Figs. 3a and b), but merge at longer periods into a simple peak (Fig. 2b).

For the two higher concentrations of AOT studied (i.e., 10^{-4} and 10^{-2} M, Figs. 2c and 2d) at around -1.0 V the central capacitance pit is transformed into a plateau of slightly higher ($6 \mu F/cm^2$) capacitance values which also shows a slow increase as the potential becomes more negative. Similar capacitance plateau neighboring with a central capacitance pit has also been observed for other micelle-forming surfactants such as SDS [29], CDBACI [30] and cholate ions [24] and has been attributed to a micellar surface film. That is, the compact film of strongly interacting adsorbate molecules is raptured into a less cohesive film consisting of surface aggregates which, in analogy with those in bulk solutions, we call surface micelles.

A less cohesive film is expected to be more conductive and thus exhibit a higher capacitance, as is indeed the case in AOT adsorption (Figs. 2c and 2d). On a molecular basis the transformation of a compact layer into AOT surface micelles can be realized by a limited break of some of the hydrogen bonds which are expected to be formed (through the $C=O$ groups) between neighboring AOT molecules in the condensed state. As the potential becomes more negative and the adsorption of AOT becomes less favored, more hydrogen bonds are broken and therefore smaller surface micelles are formed (continuous increase of the capacitance between -1.0 V and -1.5 V) until finally a sharp peak, corresponding to the dissolution of the micellar film, is observed.

The onset of the formation of this micellar film can be seen at intermediate or short times as a capacitance "hump" in Figs. 2b and 2c at c.a. -1.2 V. That is, initially small micelles (and therefore a less cohesive film) are formed, but as time elapses more H-bonds are formed resulting in a more compact micellar film which differs very little from the compact layer (collapse of the "hump" into a plateau).

An interesting point as far as the bulk CMC AOT concentration is concerned is the appearance of deformed (split) capacitance peaks at intermediate times for concentrations as low as 5×10^{-5} M (Figs. 2b and 3b). If one was to rely on these deformations (as one would have to if one used a DME of a restricted lifetime or a HMDE in a semistatic voltammetric mode) and attributed them (as was done in the past [15–19]) to the adsorption/desorption of monomers and micelles, then one should have to accept that the CMC of AOT is as low as 5×10^{-5} M, which is in contrast with the CMC determined by the surface tension data (Fig. 4).

Thus, these deformations should be treated as phase changes which occur within the interface [29, 30], and not as corresponding to the adsorption/desorption of entities already present in the bulk solution. Furthermore, the fact that these deformations vary strongly with time proves the validity of our approach by means of the 3D/ac/V in order to obtain the final, close to steady state picture of the C vs E curves.

The only correlation between the bulk CMC of AOT and the C vs. E curves recorded for long times (which is empirical and indeed very weak) is the transformation of the compact layer into a less cohesive micellar film for concentrations higher than the CMC (Fig. 2d).

Finally, we would like to comment on some of the original chronoamperometric (or more accurately, "chronocapacitometric") data that we used to reconstruct the C vs. E curves and try to interpret their features qualitatively (Figs. 5–8). In discussing these curves the C vs E curves of Fig. 2b should be our "map" as far as the final potential of the pulse is concerned.

When the potential is stepped at $+0.2$ V (Fig. 5), i.e., in the region of polylayer formation, the capacitance keeps on falling as more AOT molecules are reaching the interface and are being adsorbed. When the surface concentration of AOT reaches a critical value (after c.a. 20 s) then there occurs the phase transition of the saturated surface solution into a condensed layer or polylayer. The other curve in Fig. 5 depicts the situation when the system is stepped to 0 V (i.e., on the top of the anodic capacitance peak). At this potential the compact layer has been dissolved into a non-saturated interfacial solution which has not reached the critical concentration to be transformed into a polylayer. What we observe therefore is the intermediate between two surface states which, according to the phase transition model, has to lie on a peak and thus exhibit the high capacitance value recorded (Fig. 6).

When the potential is stepped at − 0.1 V, the region on the positive verges of the capacitance peak, there is an initial decrease in the capacitance due to a continuous diffusion of AOT molecules towards the electrode surface. However, since the completion of the first layer seems to be slow at that potential, it is likely that new AOT molecules are being deposited on top of monolayer islands, interacting with them, and forming three-dimensional aggregates which are loosely bound to the electrode and thus cause an increase in the differential capacitance with a peak at around 3 s. Such a behavior was also observed and an analogous interpretation was also given by Wandlowski and Pospišil for some imine complexes [32], and by us in the case of cetyldimethylbenzylamminium chloride [23]. As time passes though, the first layer is completed with AOT molecules and a surface state exhibiting a capacitance of c.a. $14 \mu F/cm^2$ is established, probably consisting of small surface micelles.

At − 0.2 V the other curve in Fig. 6, the situation is simpler and an induction period of c.a. 2 s is needed until the surface nuclei-aggregates ("surface micelles") reach an adequate number and size for the compact layer to start to grow through extended H-bonding and for the differential capacitance to start to decrease. Similar induction periods for the formation of the compact layer at potentials close to its negative verges are shown in Fig. 7.

Finally, Fig. 8 shows the transient resulting from a step to the top of the desorption peak (− 1.35 V) and a constant capacitance in the region where no adsorption occurs (− 1.4 V).

References

1. Aveyard R, Binks BP, Clark S, Mead J (1986) J Chem Soc Faraday Trans I 82:125
2. Hoffman H (1987) Ber Bunsenges, Phys Chem 82:988
3. Franses EI, Talmon Y, Scriven LE, Davis H.T, Miller WG (1982) J Colloid Interface Sci 86:449
4. Ruckenstein E, Nagarajan R (1977) In: Mittal KL (ed) Micellization, Solubilization and Microemulsions Vol. 1. Plenum Press, NY. P.133
5. Day RA Robinson BH, Clarke JHR, Doherty JV (1979) J Chem Soc Faraday Trans I 75: 132
6. Lalanne JR, Pouligny B, Seln E (1983) J Phys Chem 87:696
7. Jobe DJ, Reinsborough VC (1984) Can J Chem 62:280
8. Williams EF, Woodberry NT, Dixon JK (1957) J Colloid Sci 12:452
9. Rudenko SV, Averbakh KO, Smirmor OK, Levi SM (1968) Colloid J USSR (Engl Transl) 30:312
10. Fontell K (1973) J Colloid Interface Sci 44:318
11. Kilpatrick PK, Miller WG (1984) J Phys Chem 88:1649
12. Serrien G, Joos P (1990) J Colloid Interface Sci 139:149
13. Lucassen J, Drew MGB (1987) J Chem Soc Faraday Trans I 83:3093
14. Alexopoulos AH, Puig JE, Frances, EI (1989) J Colloid Interface Sci 128:26
15. Vollhardt D (1969) Colloid Polym Sci 229:15
16. Vollhardt D (1976) Colloid Polym Sci 254:64
17. Döfler HD, Müller E (1976) Tenside Deterg 13:322
18. Müller E, Döfler HD (1977) Tenside Deterg 14:75
19. Müller, E, Emons H, Döfler H.D (1981) J Colloid Interface Sci 79:567
20. Avrami M (1940) J Chem Phys 8:212
21. Buess-Herman C (1985) J Electroanal Chem 186:27
22. Papadopoulos N, Sotiropoulos S, Nikitas P (1992) J Electroanal Chem 324:375
23. Papadopoulos N, Sotiropoulos S, Nikitas P (1992) J Colloid Interface Sci 151:523
24. Papadopoulos N, Avranas A, Sotiropoulos S (1992) Bioelectrochem Bioenergetics 29:223
25. Avranas A, Papadopoulos N (1992) Langmuir 8:2804
26. Papadopoulos N (1992) Electrochim Acta 37:2447
27. Nikitas P (1992) J Electroanal Chem 329:59
28. Nikitas P, Sotiropoulos S, Papadopoulos N (1992) J Phys Chem 96:8453
29. Sotiropoulos S, Nikitas P, Papadopoulos N (1993) J Electroanal Chem 356:201.
30. Sotiropoulos S, Nikitas P, Papadopoulos N (1993) J Electroanal Chem 356:225.
31. Sathayanarayanan S, Baikerikar V (1969) J Electroanal Chem 21:2469
32. Wandlowski T, Pospišil (1989) J Electroanal Chem 258:179

Received October 15, 1993;
accepted January 18, 1994

Authors' address:

Dr. Nikos Papadopoulos
Laboratory of Physical Chemistry
Department of Chemistry
Aristotle University
54006 Thessaloniki, Greece